

# Discotic liquid crystals of transition metal complexes 29:† mesomorphism and charge transport properties of alkylthio- substituted phthalocyanine rare-earth metal sandwich complexes‡

Kazue Ban,<sup>a</sup> Kaoru Nishizawa,<sup>a</sup> Kazuchika Ohta,<sup>\*a</sup> Anick M. van de Craats,<sup>b</sup>  
John M. Warman,<sup>\*b</sup> Iwao Yamamoto<sup>a</sup> and Hirofusa Shirai<sup>a</sup>

<sup>a</sup>Department of Functional Polymer Science, Faculty of Textile Science and Technology,  
Shinshu University, Ueda 386-8567, Japan. E-mail: ko52517@giptc.shinshu-u.ac.jp

<sup>b</sup>IRI, Delft University of Technology, Mekelweg 15, 2629 JB Delft, The Netherlands.  
E-mail: warman@iri.tudelft.nl

Received 18th May 2000, Accepted 11th September 2000

First published as an Advance Article on the web 15th November 2000

A series of bis[octakis(alkylthio)phthalocyaninato]rare-earth-metal(III) discotic compounds, [(C<sub>n</sub>S)<sub>8</sub>Pc]<sub>2</sub>M (M = Eu(III), Tb(III), Lu(III); n = 8, 10, 12, 14, 16, 18), has been synthesized. The mesomorphic and supramolecular structures have been investigated by using differential scanning calorimetry, polarization microscopy and temperature-dependent X-ray diffraction techniques. From the X-ray diffraction and spectroscopic results, it was revealed that in each of the rare-earth compound classes, [(C<sub>n</sub>S)<sub>8</sub>Pc]<sub>2</sub>Eu (n = 10, 12), [(C<sub>n</sub>S)<sub>8</sub>Pc]<sub>2</sub>Tb (n = 10, 12, 14) and [(C<sub>n</sub>S)<sub>8</sub>Pc]<sub>2</sub>Lu (n = 10, 12), derivatives were found which displayed a novel unique pseudo-hexagonal mesophase.

The temperature dependence of the one-dimensional intracolumnar charge carrier mobilities, Σμ<sub>1D</sub>, has been measured for [(C<sub>12</sub>S)<sub>8</sub>Pc]<sub>2</sub>Lu and [(C<sub>18</sub>S)<sub>8</sub>Pc]<sub>2</sub>Lu using the PR-TRMC (pulse-radiolysis time-resolved microwave conductivity) technique. The mobility values in both the K and D phases are more than an order of magnitude larger than found previously for [(C<sub>12</sub>O)<sub>8</sub>Pc]<sub>2</sub>Lu and are close to the maximum values ever found for discotic materials. The lack of a decrease in Σμ<sub>1D</sub> at the mesophase to isotropic liquid transition suggests that these compounds may represent the first liquid phase organic semiconducting materials.

## 1 Introduction

Phthalocyanines have been conventionally utilized as pigments and dyes. Recently, the phthalocyaninato metal complexes have attracted attention because of their potential as photoconductor, sensor and electrode materials.<sup>2</sup>

Phthalocyaninato rare-earth metal double-decker complexes are neutral radicals. For example, bis(phthalocyaninato)lutetium(III) (hereafter abbreviated as Pc<sub>2</sub>Lu) consists of a Lu<sup>3+</sup> cation and two Pc<sup>2-</sup> anions. This complex is not charge-balanced, which makes one of the Pc macrocycles lacking in aromaticity because the number of π-electrons is not equal to 4n + 2 (n = integer: Hückel's rule). When a macrocycle is not aromatic, it is not necessarily flat. The X-ray structural analysis actually demonstrated that both of the phthalocyanine macrocycles of Pc<sub>2</sub>Lu are not coplanar but largely bent, although one of them is bent to a larger extent than the other. From these facts it was concluded that this Pc<sub>2</sub>Lu is in fact a neutral radical.<sup>3</sup> Pc rare-earth metal sandwich complexes substituted with long peripheral chains are well-known for their columnar mesophases.<sup>4</sup> These columnar mesomorphic Pc derivatives are very attractive because of their one-dimensional charge transport properties.<sup>5</sup>

Belarbi *et al.* reported the phase transitions and ac conductivities of bis[octakis(dodecyloxy)phthalocyaninato]lutetium(III) (hereafter abbreviated as [(C<sub>12</sub>O)<sub>8</sub>Pc]<sub>2</sub>Lu).<sup>6</sup> However, several problems remain unsolved in that paper. Therefore, we previously reinvestigated the phase transitions and measured the radiation-induced conductivity by using the pulse-radiolysis time-resolved microwave conductivity (PR-TRMC)

technique<sup>7</sup> for the same [(C<sub>12</sub>O)<sub>8</sub>Pc]<sub>2</sub>Lu derivative. From PR-TRMC measurements the sum of the mobilities of the holes and the electrons, Σμ<sub>TRMC</sub>, can be derived.<sup>8</sup> Because of the fast time-response and ultra-high frequency involved in this method, the mobilities obtained are thought to be intrinsic, trap-free values associated with organized domains within the material. Therefore, these mobilities can be considered to be close to the maximum value that can be obtained with well-organized, monodomain layers in electronic devices. We found higher conductivities for the [(C<sub>12</sub>O)<sub>8</sub>Pc]<sub>2</sub>Lu sandwich compound than for the corresponding non-sandwich derivatives (C<sub>n</sub>O)<sub>8</sub>PcM (M = H<sub>2</sub>, Cu, *etc.*). Moreover, a unique conductive behavior was discovered for the virgin sample which had been overlooked by Belarbi *et al.*: the conductivity rises step by step at the phase transition temperatures on heating.<sup>7</sup> Additionally, we found a novel type of D<sub>ro</sub>(P2<sub>1</sub>/a) mesophase in which two different stacking distances *h*<sub>t</sub> and *h*<sub>f</sub> were found.<sup>1</sup>

As also reported previously, alkylthio-substituted phthalocyanines, (C<sub>n</sub>S)<sub>8</sub>PcH<sub>2</sub>, and the copper complexes, (C<sub>n</sub>S)<sub>8</sub>PcCu,<sup>9</sup> display higher conductivities than their alkoxy-substituted phthalocyanines in their mesophase.<sup>8</sup> Therefore, we expected the alkylthio-substituted phthalocyanine rare-earth metal double decker complexes to also yield higher conductivity values. Hence, in this work we have synthesized this series of bis[octakis(alkylthio)phthalocyaninato]rare-earth-metal(III) double decker complexes, [(C<sub>n</sub>S)<sub>8</sub>Pc]<sub>2</sub>M (M = Eu(III), Tb(III), Lu(III); n = 8, 10, 12, 14, 16, 18), and investigated their mesomorphism and charge transport properties.

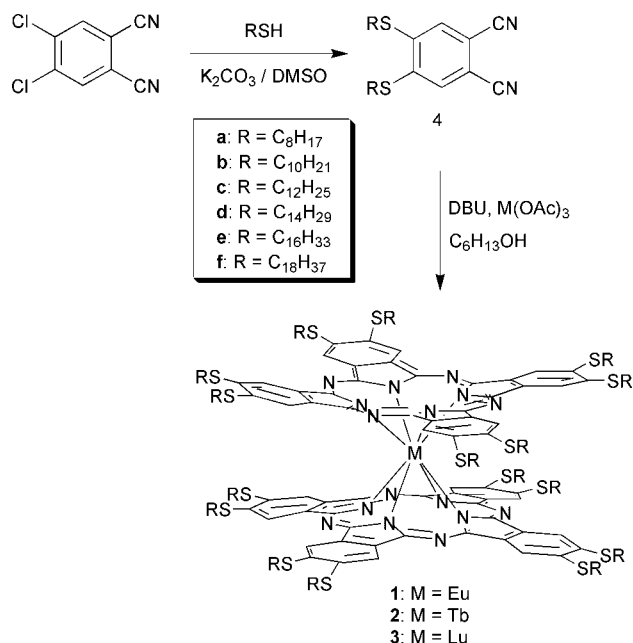
## 2 Experimental

### 2-1 Synthesis

The synthetic route is shown in Scheme 1. Since bisalkylthiophthalonitriles (**4**) could not be prepared by the

† Part 28: Ref. 1.

‡ Elemental analysis data, recrystallization solvents, yields and optical absorption spectral data for [(C<sub>n</sub>S)<sub>8</sub>Pc]<sub>2</sub>M are available as supplementary data. For direct electronic access see <http://www.rsc.org/suppdata/jm/b0/b003984p/>



**Scheme 1** Synthetic route of bis[octakis(alkylthio)phthalocyaninato]rare-earth-metal(III) complexes; M = Eu (**1a–e**), M = Tb (**2a–f**), M = Lu (**3a–f**). DBU = 1,8-diazabicyclo[5.4.0]undec-7-ene

method of Suda,<sup>10</sup> they were prepared by the method of Wöhrle.<sup>11,12</sup> Syntheses of the bis[octakis(alkylthio)phthalocyaninato]metal(III) complexes (metal = Eu, Tb, Lu; **1**, **2**, **3**) were followed using the procedures reported by us<sup>4</sup> and Belarbi *et al.*<sup>6</sup> The detailed procedures for the representative compounds, [(C<sub>12</sub>S)<sub>8</sub>Pc]<sub>2</sub>Eu (**1c**), [(C<sub>12</sub>S)<sub>8</sub>Pc]<sub>2</sub>Tb (**2c**) and [(C<sub>12</sub>S)<sub>8</sub>Pc]<sub>2</sub>Lu (**3c**) are described below.

**4,5-Bisdodecylthiophthalonitrile (4c).** A mixture of dodecane-1-thiol (2.47 g, 12.2 mmol) and 4,5-dichlorophthalonitrile (1.00 g, 5.08 mmol) in dry DMSO was heated up to 100 °C with stirring under a nitrogen atmosphere, and dry, finely powdered K<sub>2</sub>CO<sub>3</sub> was added (5 × 1.40 g, every 5 min). Then, the mixture was stirred at 100 °C for 30 min. After cooling to room temperature, it was diluted with chloroform. The organic layer was washed with water and dried over MgSO<sub>4</sub>. After removal of the solvent, the purification was carried out by recrystallization twice from *n*-hexane to give 1.89 g of solid. Yield 71%. Mps = 50.0, 55.9, 59.9–60.3 °C (solid polymorphism).

<sup>1</sup>H-NMR(CDCl<sub>3</sub>, TMS) δ 0.88(t, *J* = 5.1 Hz, 6H, CH<sub>3</sub>), 1.80–1.57(m, 40H, CH<sub>2</sub>), 3.02(t, *J* = 7 Hz, 4H, -CH<sub>2</sub>-S-), 7.41(s, 2H, Ph). IR(KBr)<sub>v<sub>max</sub></sub>/cm<sup>-1</sup> 2900(CH<sub>2</sub>), 2250(-CN).

#### Bis[octakis(dodecylthio)phthalocyaninato]europium(III)

**(1c).** A mixture of the compound **4c** (0.90 g, 1.70 mmol), europium(III) acetate tetrahydrate (0.09 g, 0.23 mmol) in hexan-1-ol (10 ml) was refluxed in the presence of 1,8-diazabicyclo[5.4.0]undec-7-ene (DBU) (0.13 g, 0.85 mmol) with stirring for 28 hours. Additional europium(III) acetate tetrahydrate (0.09 g, 0.23 mmol) and DBU (0.13 g, 0.85 mmol) were added. Then the mixture was refluxed for an additional 16 hours. After cooling to rt, the precipitate was separated by filtration and washed with methanol. The residue was purified by column chromatography (silica gel, chloroform, *R<sub>f</sub>* = 1.00), permeation chromatography (Bio-beads gel, SX-1, THF) and recrystallization twice from ethyl acetate to give 0.41 g of dark green solid.

IR(KBr)<sub>v<sub>max</sub></sub>/cm<sup>-1</sup> 2930, 2855(CH<sub>2</sub>), 1590(Ph), 750(S-CH<sub>2</sub>).

**Bis[octakis(dodecylthio)phthalocyaninato]terbium(III) (2c).** A mixture of the compound **4c** (0.78 g, 1.48 mmol), terbium(III) acetate tetrahydrate (0.08 g, 0.20 mmol) in hexan-1-ol (10 ml)

was refluxed in the presence of DBU (0.11 g, 0.74 mmol) with stirring for 16.5 hours. Additional terbium(III) acetate tetrahydrate (0.08 g, 0.20 mmol) and DBU (0.11 g, 0.74 mmol) were added. Then the mixture was refluxed for an additional 5 hours. After cooling to rt, the precipitate was separated by filtration and washed with methanol. The residue was purified by column chromatography (silica gel, chloroform, *R<sub>f</sub>* = 1.00), permeation chromatography (Bio-beads gel, SX-1, THF) and recrystallization from ethyl acetate four times to give 0.34 g of dark green solid.

IR(KBr)<sub>v<sub>max</sub></sub>/cm<sup>-1</sup> 2925, 2860(CH<sub>2</sub>), 1590(Ph), 750(S-CH<sub>2</sub>).

**Bis[octakis(dodecylthio)phthalocyaninato]lutetium(III) (3c).** A mixture of the compound **4c** (0.50 g, 0.95 mmol), lutetium(III) acetate tetrahydrate (0.06 g, 0.13 mmol) in hexan-1-ol (10 ml) was refluxed in the presence of DBU (0.07 g, 0.48 mmol) with stirring for 7 hours. Additional lutetium(III) acetate tetrahydrate (0.06 g × 2, 0.13 mmol × 2) and DBU (0.07 g × 2, 0.48 mmol × 2) were added. Then the mixture was refluxed for an additional 22 hours. After cooling to rt, the precipitate was separated by filtration and washed with methanol. The residue was purified by column chromatography (silica gel, chloroform, *R<sub>f</sub>* = 1.00), permeation chromatography (Bio-beads gel, SX-1, THF) and recrystallization from ethyl acetate four times to give 0.15 g of dark green solid.

IR(KBr)<sub>v<sub>max</sub></sub>/cm<sup>-1</sup> 2930, 2850(CH<sub>2</sub>), 1590(Ph), 745(S-CH<sub>2</sub>).

The supplementary information<sup>†</sup> lists the elemental analysis data, mass spectral data, the recrystallization solvents, and the yields of the [(C<sub>*n*</sub>S)<sub>8</sub>Pc]<sub>2</sub>M (M = Eu, **1a–e**; M = Tb, **2a–f**; M = Lu, **3a–f**) derivatives. Optical spectra of these complexes have been summarized in the supplementary information. As can be seen from this table, each of the complexes showed a Soret band, a Q band, and a “fingerprint” or “F” band at 545–575 nm which is due to the radical nature unique to the bis(phthalocyaninato)rare-earth-metal(III) sandwich complexes. Compared with the Q bands at around 700 nm, it shifts to longer wavelength in the order Lu, Tb and Eu. This is attributed to the increase in the radius of the ions.<sup>1</sup>

## 2-2 Structural characterisation

The products synthesized here were identified by <sup>1</sup>H-NMR (JEOL JNM-FX90A) and IR (Jasco A-100). Further identifications of the phthalocyanine derivatives were made by elemental analysis (Perkin-Elmer elemental analyzer 2400), MALDI-TOF mass spectra (PerSeptive Biosystems Voyager DE-Pro spectrometer), and optical absorption spectroscopy (Hitachi 330 spectrophotometer).

The phase transition behavior was observed by using a polarizing microscope (Olympus BH2), equipped with a heating plate controlled by a thermoregulator (Mettler FP80 hot stage, Mettler FP82 Central Processor), and measured by a differential scanning calorimeter (Shimadzu DSC-50). Onset temperatures in the DSC traces were determined as the phase transition temperatures. The X-ray diffraction measurements were performed with Cu-Kα radiation (Rigaku Greigerflex and Rigaku Rint) equipped with a hand-made heating plate<sup>13,14</sup> controlled by a thermoregulator.

## 2-3 PR-TRMC technique

Using the pulse-radiolysis time-resolved microwave conductivity technique (PR-TRMC) a low concentration (*ca.* 10 μM) of electron-hole pairs is produced uniformly throughout the material by a nanosecond duration pulse of 3 MeV electrons from a Van de Graaff accelerator. Since the amount of energy dissipated in the sample is accurately known from dosimetry and the energy required to produce one electron hole pair can be estimated, the concentration of charge carriers can be calculated.<sup>15</sup> This procedure, referred to as “radiation doping”,

does not perturb the primary molecular or higher order structure of the material.<sup>16</sup>

If the charge carriers formed are mobile, an increase in conductivity will occur which is monitored with nanosecond time-resolution as a decrease in the power level of microwaves which traverse the sample. The microwave circuitry has been described in detail in previous publications.<sup>8,17,18</sup> No PR-TRMC measurements could be performed above 200 °C because of limitations of the current set-up. From the change in the absolute value of the radiation-induced conductivity of the medium at the end of the pulse,  $\Delta\sigma_{\text{eop}}$ , the value of the sum of the charge carrier mobilities,  $\Sigma\mu_{\text{TRMC}}$  can be determined, since the concentration of charge carrier pairs formed in the pulse,  $N_{\text{p}}$  can be estimated (see eqn. (1) where  $e$  is the elementary charge):

$$\Delta\sigma_{\text{eop}} = eN_{\text{p}}\Sigma\mu_{\text{TRMC}} \quad (1)$$

For the samples studied in this work no attempt was made to orient the individual monodomains. The mobility value determined using eqn. (1) is therefore an effective isotropic value corresponding to random orientation of the columnar axes within microdomains. Charge transport in columnar discotic compounds is in fact known to be highly anisotropic and to occur almost exclusively along the axis of the macrocyclic stacks. Therefore all mobility values given are intracolumnar, effective one-dimensional mobilities,  $\Sigma\mu_{1\text{D}}$ , related to  $\Sigma\mu_{\text{TRMC}}$  by

$$\Sigma\mu_{1\text{D}} = 3\Sigma\mu_{\text{TRMC}} \quad (2)$$

Because of the ultra-short time scale of the measurements charge carriers are usually observed before they recombine or have time to become localised at chemical (*e.g.* O<sub>2</sub>) or physical (*e.g.* grain boundary) defects. The mobilities determined can therefore be considered to be “trap free”. The use of 30 GHz microwaves to probe the conductivity change has the added advantage over DC techniques that complications due to electrode contacts, space-charge, and domain or grain boundaries are absent. Effects due to structural disorder should also be minimised. As a result, the mobilities derived refer to the maximum value that could possibly be obtained in a DC drift experiment with a single monodomain between the electrodes. Where DC time-of-flight (TOF) measurements have proven to be possible with an orthogonally oriented sample, good agreement between the TOF and PR-TRMC mobilities has been found.<sup>19</sup> A further point worth emphasizing is that  $\Sigma\mu_{1\text{D}}$  is the sum of the positive and negative charge carrier mobilities whereas in a TOF experiment the individual mobilities can be determined.

## 3 Results and discussion

### 3-1 Mesomorphism

**3-1-1 Phase transition behavior.** In Table 1 the phase transition temperatures and corresponding enthalpy changes of the [(C<sub>n</sub>S)<sub>8</sub>Pc]<sub>2</sub>Eu ( $n=8, 10, 12, 14, 16$ ) complexes have been surveyed as measured with DSC and polarization microscopy. All europium complexes show a D<sub>h</sub> mesophase and two of the derivatives, **1b** ( $n=10$ ) and **1c** ( $n=12$ ), additionally exhibit a new mesophase M.

In Table 2 the phase transition temperatures and corresponding enthalpy changes of the [(C<sub>n</sub>S)<sub>8</sub>Pc]<sub>2</sub>Tb ( $n=8, 10, 12, 14, 16, 18$ ) complexes have been summarized. Like the europium complexes, all terbium complexes show a D<sub>h</sub> mesophase. For the three derivatives, **2b** ( $n=10$ ), **2c** ( $n=12$ ) and **2d** ( $n=14$ ), the new mesophase M was found, as for the europium complexes.

**Table 1** Phase transition temperatures and enthalpy changes data of the [(C<sub>n</sub>S)<sub>8</sub>Pc]<sub>2</sub>Eu ( $n=8, 10, 12, 14, 16$ ) derivatives<sup>a</sup>

Complex	Phase	$T/\text{°C} [\Delta H/\text{kJ mol}^{-1}]$	Phase
$n=8$ ( <b>1a</b> )	K	98[118]	D <sub>h</sub> $\xleftrightarrow{252[13.1]}$ I.L.
$n=10$ ( <b>1b</b> )	X	$\xleftarrow{-1[17.8]}$ M $\xleftrightarrow{68[11.9]}$ D <sub>h</sub> $\xleftrightarrow{209[8.92]}$ I.L.	
$n=12$ ( <b>1c</b> )	X	$\xleftarrow{22[50.3]}$ M $\xleftrightarrow{64[9.89]}$ D <sub>h</sub> $\xleftrightarrow{181[14.3]}$ I.L.	
$n=14$ ( <b>1d</b> )	X	$\xleftarrow{13[93.0]}$ D <sub>h</sub> $\xleftrightarrow{152[11.3]}$ I.L.	
$n=16$ ( <b>1e</b> )	K	$\xleftrightarrow{50[166.2]}$ D <sub>h</sub> $\xleftrightarrow{134[12.9]}$ I.L.	

<sup>a</sup>Phase nomenclature: K=crystal, D<sub>h</sub>=discotic hexagonal columnar mesophase, I. L.=isotropic liquid; X is an unidentified phase because of the limit of the instrument, M=new mesophase: see the main text.

**Table 2** Phase transition temperatures and enthalpy changes data of the [(C<sub>n</sub>S)<sub>8</sub>Pc]<sub>2</sub>Tb ( $n=8, 10, 12, 14, 16, 18$ ) derivatives<sup>a</sup>

Complex	Phase	$T/\text{°C} [\Delta H/\text{kJ mol}^{-1}]$	Phase
$n=8$ ( <b>2a</b> )	K	$\xleftrightarrow{102[126.7]}$ D <sub>h</sub> $\xleftrightarrow{242[13.2]}$ I.L.	
$n=10$ ( <b>2b</b> )	X	$\xleftrightarrow{3[20.5]}$ M $\xleftrightarrow{56[23.4]}$ D <sub>h</sub> $\xleftrightarrow{205[12.1]}$ I.L.	
$n=12$ ( <b>2c</b> )	X	$\xleftrightarrow{0-20[55.9]}$ M $\xleftrightarrow{53[7.6]}$ D <sub>h</sub> $\xleftrightarrow{172[9.6]}$ I.L.	
$n=14$ ( <b>2d</b> )	X	$\xleftrightarrow{22}$ M $\xleftrightarrow{47[6.3]}$ D <sub>h</sub> $\xleftrightarrow{144[12.6]}$ I.L. K <sub>1</sub> $\xleftrightarrow{37}$ M	
$n=16$ ( <b>2e</b> )	K	$\xleftrightarrow{46[133.1]}$ D <sub>h</sub> $\xleftrightarrow{132[13.5]}$ I.L.	
$n=18$ ( <b>2f</b> )	K <sub>1</sub>	$\xleftrightarrow{33}$ D <sub>h</sub> $\xleftrightarrow{116[12.3]}$ I.L. K <sub>2</sub> $\xleftrightarrow{57}$ D <sub>h</sub>	

<sup>a</sup>Phase nomenclature: K=crystal, D<sub>h</sub>=discotic hexagonal columnar mesophase, I. L.=isotropic liquid; X is an unidentified phase because of the limit of the instrument, M=new mesophase: see the main text. The phases for which no enthalpy changes are given, could not be obtained in pure form.

In Table 3 the phase transition temperatures and the corresponding enthalpy changes of the [(C<sub>n</sub>S)<sub>8</sub>Pc]<sub>2</sub>Lu ( $n=8, 10, 12, 14, 16, 18$ ) complexes have been summarized. When the virgin crystal K<sub>3v</sub> of [(C<sub>8</sub>S)<sub>8</sub>Pc]<sub>2</sub>Lu (**3a**) was heated at 10 °C min<sup>-1</sup> from rt, it transformed into a hexagonal columnar (D<sub>h</sub>) mesophase at 89 °C showing a large endothermic peak. On further heating, the D<sub>h</sub> mesophase cleared into an isotropic liquid (I.L.) at 219 °C. When the I.L. was cooled down at -10 °C min<sup>-1</sup>, another crystalline phase K<sub>1</sub> different from the virgin crystalline phase, appeared. When the polycrystalline K<sub>1</sub> phase was heated, it transformed into a K<sub>2</sub> crystalline phase at 45 °C. On further heating, this K<sub>2</sub> crystalline phase melted into the D<sub>h</sub> mesophase at 84 °C. It cleared at 219 °C just as the virgin sample did.

The [(C<sub>10</sub>S)<sub>8</sub>Pc]<sub>2</sub>Lu (**3b**) derivative showed an unidentified phase X below rt, and [(C<sub>12</sub>S)<sub>8</sub>Pc]<sub>2</sub>Lu (**3c**) showed a crystalline phase K at rt. Both the decylthio and dodecylthio derivatives

**Table 3** Phase transition temperatures and enthalpy changes data of the  $[(C_nS)_8Pc]_2Lu$  ( $n=8, 10, 12, 14, 16, 18$ ) derivatives<sup>a</sup>

Complex	Phase	$T/^\circ C$ [ $\Delta H/ kJ mol^{-1}$ ]	Phase
$n=8$ (3a)	$K_1$	45[29.7]	$K_2$
	$K_2$	84[23.6]	$D_h$
	$D_h$	219[17.5]	I.L.
$n=10$ (3b)	X	6[17.6]	M
	M	40[11.1]	$D_h$
	$D_h$	192[12.4]	I.L.
$n=12$ (3c)	K	27[55.1]	M
	M	38[4.2]	$D_h$
	$D_h$	167[11.5]	I.L.
$n=14$ (3d)	K	38[123.5]	$D_h$
	$D_h$	146[14.1]	I.L.
$n=16$ (3e)	K	46[176.5]	$D_h$
	$D_h$	126[8.12]	I.L.
$n=18$ (3f)	$K_1$	32	$K_2$
	$K_2$	53[251] <sup>b</sup>	$D_h$
	$D_h$	110[6.02]	I.L.

<sup>a</sup>Phase nomenclature: K = crystal,  $D_h$  = discotic hexagonal columnar mesophase, I. L. = isotropic liquid; X is an unidentified phase because of the limit of the instrument, M = new mesophase: see the main text. <sup>b</sup>This enthalpy change is the sum of two phase transitions,  $K_1 \rightarrow K_2$ , and  $K_2 \rightarrow D_h$ , because the corresponding peaks in the DSC thermogram could not be analyzed separately.

(3b and 3c) transformed into the new mesophase M at 6 °C and 27 °C, respectively. This M phase did not appear for the other lutetium complexes and transformed into a  $D_h$  mesophase with a broad endothermic peak at 40 °C (for 3b) and 38 °C (for 3c). The M phase will be described in detail below.

In Fig. 1, the phase transition temperatures of the Eu, Tb and Lu complexes are plotted as a function of the number of carbon atoms in the alkylthio chains ( $n$ ). Although each of the metal complexes shows very similar phase transitions, the Eu complexes exhibit the widest temperature range for the mesophases. The new mesophase M has only been found for decylthio and dodecylthio metal complexes ( $n=10,12$ ) and for one tetradecylthio compound, namely the terbium complex  $[(C_{14}S)_8Pc]_2Tb$  (2d). When the highest melting points are connected by a line, a very smooth curve was found for all compound series. From these smooth curves, it can be deduced that the unidentified X phase is a crystalline phase.

**3-1-2 Identification of the mesophases.** Identification of the mesophases was carried out by X-ray diffraction measurements and microscopic observations of the textures. The X-ray data of the Eu, Tb and Lu complexes have been summarized in Tables 4, 5, and 6, respectively. The M phase of  $[(C_{14}S)_8Pc]_2Tb$  could not be submitted to the X-ray diffraction structure analysis, because its mesophase exists at rt and the M– $D_h$  phase transition temperature is too close to rt to prevent the phase transition to  $D_h$  during the measurement.

All higher temperature mesophases could be identified by X-ray diffraction measurements at 100–125 °C. These gave three to seven sharp peaks in the small angle region with spacings in the ratio of  $1:1/\sqrt{3}:1/2$ : etc. Hence, all higher temperature mesophases could be assigned to hexagonal columnar mesophases,  $D_h$ . The  $[(C_{12}S)_8Pc]_2Tb$  derivative exhibited textures of hexagons and snow-flakes typical of a  $D_h$  mesophase, as shown in Fig. 2. Each of the textures has a six-fold axis which is a characteristic for a  $D_h$  mesophase. Hence, these textures bear out the identification by X-ray diffraction studies. In the X-ray large angle region, two peaks due to the stacking distances  $h_1$  and  $h_2$  in the columns could be observed. The details will be discussed below.

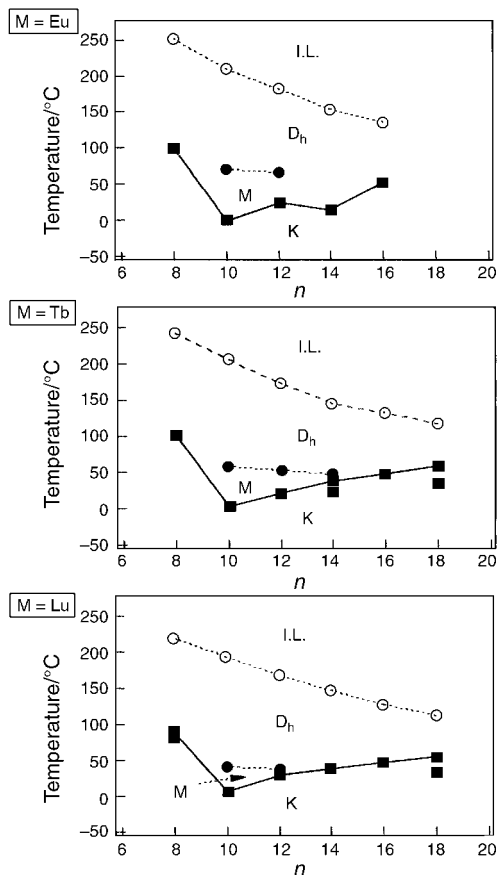


**Fig. 1** Phase transition temperatures as a function of the number of carbon atoms in the alkylthio chains ( $n$ ) for all the  $[(C_nS)_8Pc]_2M$  derivatives.

All metal complexes gave a new mesophase M for  $n=10,12$  in the lower temperature region. As shown in Fig. 3, the X-ray diffraction data of the representative  $[(C_{12}S)_8Pc]_2Eu$  derivative are drawn as circles on a two-dimensional hexagonal reciprocal lattice (Hex  $a^*$  vs. Hex  $a^*$ ) superimposed with a rectangular reciprocal lattice (Rec  $a^*$  vs. Rec  $b^*$ ) having a relationship of  $a=\sqrt{3}b$ . Peak No. 12 is broad and assigned to the molten alkylthio chains. The sharp peak No. 13 ( $d=3.30 \text{ \AA}$ ) corresponds to the usual stacking distance between the cofacially stacked Pc disks. Peaks No. 12 and No. 13 were therefore excluded in the 2D-column-packing structure analysis. All of the peaks Nos. 1, 3, 4, 5, 6, 8, 10 and 11 fit very well with a 2D-hexagonal reciprocal lattice, Hex  $a^*$  vs. Hex  $a^*$ . However, peaks, Nos. 2, 7 and 9 do not fit. On the other hand, peaks from 1 to 11 fit very well to a 2D-rectangular reciprocal lattice, Rec  $a^*$  vs. Rec  $b^*$ . If this mesophase was a conventional rectangular ordered columnar  $D_{ro}$  mesophase, it should have a relationship of  $a \neq \sqrt{3}b$  and  $h=ca. 4.7 \text{ \AA}$  as illustrated in Fig. 3(a). Since the present M phase has a relationship of  $a=\sqrt{3}b$  and  $h=3.3 \text{ \AA}$ , it must not be a conventional  $D_{ro}$  mesophase. Moreover, since a conventional hexagonal ordered columnar ( $D_{ho}$ ) mesophase has a relationship of  $a=\sqrt{3}b$  and  $h=ca.3.5 \text{ \AA}$ , it is likely to be applicable for this M phase. However, peak Nos. 2, 7 and 9 should not appear for such a conventional  $D_{ho}$  mesophase. Hence, this M phase is a unique novel mesophase having both characteristics of  $D_{ho}$  and  $D_{ro}$  ones.

In 1991, Guillon and co-workers found a pseudo-hexagonal columnar (Pseudo  $D_h$ ) mesophase for a Pc-based discotic liquid crystal.<sup>20</sup> In this pseudo  $D_h$  mesophase, the tilted cores have a rectangular lattice, whereas the whole molecules have a 2D-hexagonal lattice, as illustrated in Fig. 3(b). This Pseudo  $D_h$  structure has a relationship of  $a=\sqrt{3}b$  and  $h=ca.4.7 \text{ \AA}$ . It cannot be adopted for the present M phase, because the shorter

**Table 4** X-Ray data of the  $[C_nS]_8Pc]_2Eu$  ( $n=8, 10, 12, 14, 16$ ) derivatives

Complex (mesophase)	Lattice constant /Å	Spacing /Å		Miller indices ( $h k l$ )			
		Observed	Calculated		Hex	Rec	
			Hex	Rec			
<b>1a:</b> $[C_8S]_8Pc]_2Eu$ ( $D_h$ at 120 °C)	$a=27.9$ $h_2=ca.7.3$ $h_1=ca.3.6$	24.5	24.2	(100)			
		14.0	14.0	(110)			
		12.1	12.1	(200)			
		9.17	9.14	(210)			
		7.92	8.06	(300)			
		ca. 7.3	—	$h_2$			
		6.70	6.71	$a$ (310)			
		ca. 4.7	—	$a$			
		ca. 3.6	—	$h_1$			
		<b>1b:</b> $[C_{10}S]_8Pc]_2Eu$ ( $M$ at 50 °C)	Hex $a=31.9$ $h_2=6.90$ $h_1=ca.3.3$ Rec $a=55.2$ $b=31.9$ =hex $a$ $h_2=6.90$ $h_1=ca.3.3$	27.2	27.6	27.6	(100)
20.8	—			—20.9	—	(210)	
15.9	15.9			15.9	(110)	(020)(310)	
13.7	13.8			13.8	(200)	(220)(400)	
12.2	—			12.0	—	(320)	
10.5	10.4			10.4	(210)	(420)(510)	
9.21	9.20			9.20	(300)	(330)(600)	
8.04	7.96			7.96	(220)	(040)(620)	
7.74	7.65			7.65	(310)	(240)(530)	
6.90	6.90			6.90	(400) + $h_2$	$a$ (440) + $h_2$	
ca. 4.6	—			—	$a$	$a$	
4.28	—			4.32	—	(470)	
ca. 3.3	—			—	$h_1$	$h_1$	
<b>1b:</b> $[C_{10}S]_8Pc]_2Eu$ ( $D_h$ at 120 °C)	$a=29.9$ $h_2=7.23$			25.5	25.9	(100)	
		14.9	14.9	(110)			
		12.9	12.9	(200)			
		9.82	9.79	(210)			
		8.67	8.63	(300) + $h_2$			
		7.23	7.18	(130)			
		6.08	5.94	(320)			
		ca.4.7	—	$a$			
<b>1c:</b> $[C_{12}S]_8Pc]_2Eu$ ( $M$ at 45 °C)	Hex $a=34.0$ $h_2=7.43$ $h_1=3.30$ Rec $a=58.9$ $b=34.0$ =hex $a$ $h_2=7.43$ $h_1=3.30$	28.8	29.5	29.5	(100)	(110)(200)	
		22.0	—	22.3	—	(210)	
		17.0	17.0	17.0	(110)	(020)(310)	
		14.8	14.7	14.7	(200)	(220)(400)	
		11.2	11.1	11.1	(210)	(310)(420)	
		9.85	9.82	9.82	(300)	(330)(600)	
		9.45	—	9.43	—	(610)	
		8.25	8.17	8.17	(310)	(240)	
		7.74	—	7.80	—	(340)	
		7.43	7.36	7.42	(400) + $h_2$	(630) + $h_2$	
		5.65	5.67	5.67	(330)	$a$ (060)	
		ca. 4.5	—	—	$a$	$a$	
3.30	—	—	$h_1$	$h_1$			
<b>1c:</b> $[C_{12}S]_8Pc]_2Eu$ ( $D_h$ at 120 °C)	$a=31.8$ $h_2=ca.7.2$	27.0	27.5				
		15.9	15.9	(100)			
		13.7	13.8	(110)			
		10.5	10.4	(200)			
		9.23	9.17	(210)			
		7.52	7.63	(300)			
		ca.7.2	—	(310)			
		ca.4.7	—	$h_2$			
				$a$			
<b>1d:</b> $[C_{14}S]_8Pc]_2Eu$ ( $D_h$ at 120 °C)	$a=34.2$ $h_2=ca.7.6$ $h_1=ca.3.5$	29.8	29.6	(100)			
		17.1	17.1	(110)			
		15.0	14.8	(200)			
		11.1	11.2	(210)			
		8.08	8.22	(310)			
		ca.7.6	—	$h_2$			
		5.39	5.32	$a$ (510)			
		ca.4.8	—	$a$			
ca.3.5	—	$h_1$					
<b>1e:</b> $[C_{16}S]_8Pc]_2Eu$ ( $D_h$ at 120 °C)	$a=34.3$ $h_2=ca.7.7$	29.7	29.7	(100)			
		16.9	17.2	(110)			
		15.2	14.9	(200)			
		10.2	9.90	(300)			
		ca.7.7	—	$h_2$			
		ca.4.6	—	$a$			

<sup>a</sup>Halo of the molten alkylthio chains.

**Table 5** X-Ray data of the [(C<sub>n</sub>S)<sub>8</sub>Pc]<sub>2</sub>Tb (*n* = 8, 10, 12, 14, 16, 18) derivatives

Complex (mesophase)	Lattice constant /Å	Spacing /Å			Miller indices ( <i>h k l</i> )	
		Observed	Calculated		Hex	Rec
			Hex	Rec		
<b>2a:</b> [(C <sub>8</sub> S) <sub>8</sub> Pc] <sub>2</sub> Tb (D <sub>h</sub> at 120°C)	<i>a</i> = 27.9 <i>h</i> <sub>2</sub> = <i>ca.</i> 7.4	24.1 14.0 12.4 9.07 7.94 <i>ca.</i> 7.4 6.55 5.43 <i>ca.</i> 4.7	24.1 14.0 12.1 9.11 8.04 — 6.69 5.53 —	27.3 20.6 15.7 13.6 10.3 9.09 7.56 — — —	(100) (110) (200) (210) (300) <i>h</i> <sub>2</sub> (310) (230) <i>a</i>	
<b>2b:</b> [(C <sub>10</sub> S) <sub>8</sub> Pc] <sub>2</sub> Tb (M at 40°C)	Hex <i>a</i> = 31.5 <i>h</i> <sub>2</sub> = <i>ca.</i> 6.5 <i>h</i> <sub>1</sub> = 3.27 Rec <i>a</i> = 54.5 <i>b</i> = 31.5 = hex <i>a</i> <i>h</i> <sub>2</sub> = <i>ca.</i> 6.5 <i>h</i> <sub>1</sub> = 3.27	27.0 20.7 15.7 13.7 10.4 9.27 7.62 <i>ca.</i> 6.5 6.01 5.53 <i>ca.</i> 4.5 3.27	27.3 — 15.7 13.6 10.3 9.09 7.56 — 5.95 5.45 — —	27.3 20.6 15.7 13.6 10.3 9.01 7.56 — 5.95 5.45 — —	(100) — (110) (200) (210) (300) (310) <i>h</i> <sub>2</sub> (410) — <i>a</i> <i>h</i> <sub>1</sub>	(110)(200) (210) (020)(310) (220)(400) (130) (330)(600) (240) <i>h</i> <sub>2</sub> (350) (550) <i>a</i> <i>h</i> <sub>1</sub>
<b>2b:</b> [(C <sub>10</sub> S) <sub>8</sub> Pc] <sub>2</sub> Tb (D <sub>h</sub> at 120°C)	<i>a</i> = 29.4 <i>h</i> <sub>2</sub> = 7.31	25.1 14.7 12.9 9.74 8.48 7.31 6.42 <i>ca.</i> 4.7	25.5 14.7 12.7 9.62 8.48 7.34 6.36 —	— — — — — — — —	(100) (110) (200) (210) (300) (220) + <i>h</i> <sub>2</sub> (400) <i>a</i>	
<b>2c:</b> [(C <sub>12</sub> S) <sub>8</sub> Pc] <sub>2</sub> Tb (M at 40°C)	Hex <i>a</i> = 34.1 <i>h</i> <sub>2</sub> = 6.50 <i>h</i> <sub>1</sub> = 3.29 Rec <i>a</i> = 59.1 <i>b</i> = 34.1 = hex <i>a</i> <i>h</i> <sub>2</sub> = 6.50 <i>h</i> <sub>1</sub> = 3.29	29.1 22.2 17.1 14.7 11.3 9.82 8.28 6.50 <i>ca.</i> 4.4 3.29	29.5 — 17.1 14.8 11.2 9.85 8.20 6.45 — —	29.5 22.3 17.1 14.8 11.2 9.85 8.19 6.45 — —	(100) — (110) (200) (210) (300) (310) (410) + <i>h</i> <sub>2</sub> <i>a</i> <i>h</i> <sub>1</sub>	(110)(200) (210) (020)(310) (220)(400) (420) (330) (530)(240) (350) + <i>h</i> <sub>2</sub> <i>a</i> <i>h</i> <sub>1</sub>
<b>2c:</b> [(C <sub>12</sub> S) <sub>8</sub> Pc] <sub>2</sub> Tb (D <sub>h</sub> at 120°C)	<i>a</i> = 31.4 <i>h</i> <sub>2</sub> = <i>ca.</i> 7.4	27.2 15.9 13.7 9.17 <i>ca.</i> 7.4 5.62 <i>ca.</i> 4.7 3.91	27.2 15.9 13.7 9.08 — 5.45 — 3.89	— — — — — — — —	(100) (110) (200) (300) <i>h</i> <sub>2</sub> (500) <i>a</i> (350)	
<b>2d:</b> [(C <sub>14</sub> S) <sub>8</sub> Pc] <sub>2</sub> Tb (D <sub>h</sub> at 120°C)	<i>a</i> = 33.5 <i>h</i> <sub>2</sub> = <i>ca.</i> 7.6	29.0 16.8 14.3 11.0 9.57 8.13 <i>ca.</i> 7.6 <i>ca.</i> 4.7	29.0 16.8 14.5 11.0 9.68 8.05 — —	— — — — — — — —	(100) (110) (200) (210) (300) (130) <i>h</i> <sub>2</sub> <i>a</i>	
<b>2e:</b> [(C <sub>16</sub> S) <sub>8</sub> Pc] <sub>2</sub> Tb (D <sub>h</sub> at 120°C)	<i>a</i> = 34.6 <i>h</i> <sub>2</sub> = <i>ca.</i> 7.4	29.9 17.7 15.3 11.7 8.50 <i>ca.</i> 7.4 6.81 <i>ca.</i> 4.7	29.9 17.3 15.0 11.3 8.64 — 6.87 —	— — — — — — — —	(100) (110) (200) (210) (220) <i>h</i> <sub>2</sub> (230) <i>a</i>	
<b>2f:</b> [(C <sub>18</sub> S) <sub>8</sub> Pc] <sub>2</sub> Tb (D <sub>h</sub> at 80°C)	<i>a</i> = 38.2 <i>h</i> <sub>2</sub> = <i>ca.</i> 7.0 <i>h</i> <sub>1</sub> = <i>ca.</i> 3.5	33.1 19.2 16.6 12.7 9.61	33.1 19.1 16.6 12.5 9.56	— — — — —	(100) (110) (200) (210) (220)	

**Table 5** X-Ray data of the [(C<sub>n</sub>S)<sub>8</sub>Pc]<sub>2</sub>Tb (*n* = 8, 10, 12, 14, 16, 18) derivatives (Continued)

Complex (mesophase)	Lattice constant /Å	Spacing /Å		Miller indices ( <i>h k l</i> )		
		Observed	Calculated		Hex	Rec
			Hex	Rec		
		<i>ca.</i> 7.0	—		<i>h</i> <sub>2</sub>	
		6.41	6.37		(330)	
		<i>ca.</i> 4.5	—		<i>a</i>	
		<i>ca.</i> 3.5	—		<i>h</i> <sub>1</sub>	

<sup>a</sup>Halo of the molten alkylthio chains.

stacking distance  $h = 3.3 \text{ \AA}$  could not be explained for such tilted cores in the Pseudo D<sub>h</sub> mesophase. Therefore, in this M phase, non-tilted cores have a hexagonal lattice, whereas the whole molecules have a rectangular lattice as illustrated in Fig. 3(c).

In our previous work, we found a new type of rectangular mesophase, D<sub>ro</sub>(P2<sub>1</sub>/a), for bis[octakis(dodecyloxy)phthalocyaninato]lutetium,<sup>1</sup> as illustrated in Fig. 4(2). It is highly interesting that this mesophase gives both the stacking distance of 3.3 Å for non-tilted cores and the 4.1 Å for tilted cores. Since the present M mesophase does not show the stacking distance at 4.1 Å, it is apparent that this M phase is not the new type of D<sub>ro</sub>(P2<sub>1</sub>/a) mesophase.

Therefore, we propose a new model for the M mesophase, which is illustrated in Fig. 4(3): the central Pc cores stack regularly face-to-face and form a 2D-hexagonal lattice, whereas the whole molecules form a 2D-rectangular lattice having a relationship  $a = \sqrt{3}b$ . For this model, the Pc cores and whole molecules give reflections from the hexagonal lattice and rectangular lattice, respectively. This model can explain all the reflections of the M mesophase. Hence, this M phase is identified as a novel pseudo-hexagonal mesophase. Fig. 4(1) and (3) illustrate the conventional pseudo-hexagonal mesophase found by Guillon's group and the novel pseudo-hexagonal mesophase found by us, respectively. Hence, there are three different mesophases having a relationship of  $a = \sqrt{3}b$ , as illustrated in Fig. 4(1), (3) and (4). To distinguish them, we propose a new nomenclature denoted in the right part of Fig. 4. If the whole molecules have a 2D-hexagonal lattice and the cores have a 2D-rectangular lattice, it is denoted as D<sub>hr</sub> or D<sub>hr</sub>(P2<sub>1</sub>/a) together with the full symmetries, as in Fig. 4(1). If necessary for further notation of the stacking order in the column, it should be denoted as D<sub>hro</sub>(P2<sub>1</sub>/a) and D<sub>hrd</sub>(P2<sub>1</sub>/a) for ordered columns and disordered columns, respectively. According to this rule, in which the symmetries from the whole molecule to central core should be denoted from left to right, the new pseudo-hexagonal mesophase is noted as D<sub>rh</sub>(P2<sub>1</sub>/a), corresponding to Fig. 4(3). The conventional D<sub>h</sub> mesophase in Fig. 4(4) should be denoted as D<sub>hh</sub> according to this new nomenclature.

Fig. 5 gives schematic representations of the mesophase structure changes for the [(C<sub>n</sub>S)<sub>8</sub>Pc]<sub>2</sub>M (M = Eu, Tb, Lu and *n* = 10, 12) derivatives on heating. As can be seen from this figure, the tilted molecules become stepwise cofacially stacked on heating.

**3-1-3 Intracolumnar stacking distances.** As can be seen from Tables 4–6, some of the shorter chain alkylthio-substituted complexes clearly show at lower temperature two stacking distances between double-deckers at *ca.* 7 Å (*h*<sub>2</sub>) and single-deckers at *ca.* 3.5 Å (*h*<sub>1</sub>). The stacking distance at *ca.* 3.5 Å has been attributed to rapid thermal fluctuations of the conformations of the disks which extinguish the difference between the upper and lower disks in the double-decker. If the difference would be perfect, the stacking distance of *ca.* 3.5 Å (*h*<sub>1</sub>) would not have been observed in the X-ray diffraction patterns.

Thermal fluctuations may cause trampoline movements of the Pc disks. As mentioned in the introductory part, one of the Pc disks in the double-decker has a radical nature. Hence, the Pc disk bends just like a dome. On increasing the temperature, the trampoline movement of the dome may occur faster to give apparent single-deckers on the time average.

Fig. 6 shows the X-ray diffraction patterns of the [(C<sub>12</sub>S)<sub>8</sub>Pc]<sub>2</sub>Lu complex of the D<sub>rh</sub>(P2<sub>1</sub>/a) mesophase at 33 °C and the D<sub>hh</sub> mesophase at 45 °C and 155 °C. As can be seen from this figure, the two intracolumnar stacking distances, *h*<sub>1</sub> and *h*<sub>2</sub>, become less intense, broader and longer with increasing temperature. Especially the *h*<sub>1</sub> stacking distance is sensitive to temperature changes. This is attributed to the increasing disorder and the expansion of the stacking distance between the disks with increasing temperature.

### 3-2 Charge carrier mobilities

The PR-TRMC technique has been used to investigate the charge transport properties of the [(C<sub>n</sub>S)<sub>8</sub>Pc]<sub>2</sub>Lu compounds with *n* = 12 and 18 and the values of the one-dimensional, intracolumnar mobility found,  $\Sigma\mu_{1D}$ , are shown as a function of temperature in Fig. 7. As can be seen,  $\Sigma\mu_{1D}$  is only weakly dependent on temperature apart from an abrupt decrease by a factor of approximately 3 at the transition from the crystalline solid to the D<sub>h</sub> mesophase. Such a pronounced decrease at a K→D transition has been observed in other discotic materials and is attributed to melting of the hydrocarbon chains with a resulting increase in the disorder within the columns.<sup>8</sup> This behaviour is also displayed by the monomeric metal-free and copper substituted octakis-alkylthio-Pc derivatives the results of which are shown for comparison in Fig. 8. The absolute values of  $\Sigma\mu_{1D}$  in the D<sub>h</sub> phases of the dimeric and monomeric octakis-alkylthio-Pc compounds shown in Fig. 7 and 8 are also seen to be very similar, with all of them lying within the range of 0.15 to 0.35 cm<sup>2</sup> V<sup>-1</sup> s<sup>-1</sup>.

These mobility values are close to an order of magnitude larger than the value of *ca.* 0.04 cm<sup>2</sup> V<sup>-1</sup> s<sup>-1</sup> found for the D<sub>h</sub> phase of octaalkoxy substituted materials.<sup>8,15</sup> The pronounced positive effect on the charge transport properties of sulfur compared with oxygen as chain-to-core coupling element is attributed to the larger size of the sulfur atom which hinders rotational and translational displacements of the macrocycles within the cores of the columns. The resulting decrease in structural disorder within the stacks of the octakis-alkylthio compounds is favorable for rapid charge transport. The mesophase values of  $\Sigma\mu_{1D}$  for the present compounds are in fact close to the maximum values previously obtained for discotic materials, *i.e.* *ca.* 0.4 cm<sup>2</sup> V<sup>-1</sup> s<sup>-1</sup> for hexaalkyl substituted hexabenzocoronenes.<sup>21</sup>

It is of interest that the presence of a central metal atom appears to have little influence on the charge transport properties in the mesophase even in the case of the present free radical dimers. The excess electronic charge appears therefore to be associated completely with the aromatic  $\pi$ -electron system of the phthalocyanine macrocycles and the rate

**Table 6** X-Ray data of the [(C<sub>n</sub>S)<sub>8</sub>Pc]<sub>2</sub>Lu (*n* = 8, 10, 12, 14, 16) derivatives.

Complex	Lattice constant /Å	Spacing /Å			Miller indices ( <i>h k l</i> )	
		Observed	Calculated		Hex	Rec
			Hex	Rec		
<b>3a:</b> [(C <sub>8</sub> S) <sub>8</sub> Pc] <sub>2</sub> Lu (D <sub>h</sub> at 125 °C)	<i>a</i> = 26.4	22.7	22.9	(100)		
	<i>h</i> <sub>2</sub> = <i>ca.</i> 6.2	13.2	13.2	(110)		
	<i>h</i> <sub>1</sub> = <i>ca.</i> 3.6	11.4	11.4	(200)		
		8.64	8.53	(210)		
		<i>ca.</i> 6.2	—	<i>h</i> <sub>2</sub>		
		<i>ca.</i> 4.7	—	<i>a</i>		
		<i>ca.</i> 3.6	—	<i>h</i> <sub>1</sub>		
<b>3b:</b> [(C <sub>10</sub> S) <sub>8</sub> Pc]Lu (M at rt)	Hex	26.6	27.1	27.1	(100)	(110)(200)
	<i>a</i> = 31.3	21.0	—	20.5	—	(210)
	<i>h</i> <sub>2</sub> = <i>ca.</i> 7.6	15.6	15.6	15.6	(110)	(020)(310)
	<i>h</i> <sub>1</sub> = 3.28	13.6	13.5	13.6	(200)	(220)(400)
	Rec	10.3	10.2	10.2	(210)	(420)(510)
	<i>a</i> = 54.2	<i>ca.</i> 7.6	—	—	<i>h</i> <sub>2</sub>	<i>h</i> <sub>2</sub>
	<i>b</i> = 31.3	<i>ca.</i> 4.3	—	—	<i>a</i>	<i>a</i>
	= hex <i>a</i>	3.28	—	—	<i>h</i> <sub>1</sub>	<i>h</i> <sub>1</sub>
	<i>h</i> <sub>2</sub> = <i>ca.</i> 7.6					
	<i>h</i> <sub>1</sub> = 3.28					
<b>3b:</b> [(C <sub>10</sub> S) <sub>8</sub> Pc] <sub>2</sub> Lu (D <sub>h</sub> at 120 °C)	<i>a</i> = 29.0	25.1	25.1	(100)		
	<i>h</i> <sub>2</sub> = <i>ca.</i> 6.7	14.5	14.5	(110)		
		12.6	12.5	(200)		
		9.51	9.48	(210)		
		8.47	8.36	(300)		
		<i>ca.</i> 6.7	—	<i>h</i> <sub>2</sub>		
		<i>ca.</i> 4.7	—	<i>a</i>		
<b>3c:</b> [(C <sub>12</sub> S) <sub>8</sub> Pc] <sub>2</sub> Lu (M at 32 °C)	Hex	29.1	29.2	29.2	(100)	(110)(200)
	<i>a</i> = 33.8	22.5	—	22.1	—	(210)
	<i>h</i> <sub>2</sub> = <i>ca.</i> 6.5	16.8	16.9	16.9	(110)	(020)(310)
	<i>h</i> <sub>1</sub> = 3.28	14.7	14.6	14.6	(200)	(220)(400)
	Rec	11.2	11.0	11.3	(210)	(420)(510)
	<i>a</i> = 58.4	9.88	9.74	9.74	(300)	(330)(600)
	<i>b</i> = 33.8	8.26	8.10	8.35	(310)	(140)
	= hex <i>a</i>	7.42	7.31	7.37	(400)	(630)
	<i>h</i> <sub>2</sub> = <i>ca.</i> 6.5	<i>ca.</i> 6.5	—	—	<i>h</i> <sub>2</sub>	<i>h</i> <sub>1</sub>
	<i>h</i> <sub>1</sub> = 3.28	<i>ca.</i> 4.4	—	—	<i>a</i>	<i>a</i>
	3.28	—	—	<i>h</i> <sub>1</sub>	<i>h</i> <sub>2</sub>	
<b>3c:</b> [(C <sub>12</sub> S) <sub>8</sub> Pc] <sub>2</sub> Lu (D <sub>h</sub> at 120 °C)	<i>a</i> = 30.7	26.6	26.6	(100)		
	<i>h</i> <sub>2</sub> = <i>ca.</i> 7.0	15.5	15.5	(110)		
		13.4	13.4	(200)		
		10.2	10.2	(210)		
		7.73	7.73	(220)		
		<i>ca.</i> 7.0	—	<i>h</i> <sub>2</sub>		
		<i>ca.</i> 4.7	—	<i>a</i>		
<b>3d:</b> [(C <sub>14</sub> S) <sub>8</sub> Pc] <sub>2</sub> Lu (D <sub>h</sub> at 120 °C)	<i>a</i> = 32.9	27.8	28.5	(100)		
	<i>h</i> <sub>2</sub> = <i>ca.</i> 7.8	16.5	16.5	(110)		
		14.2	14.3	(200)		
		10.8	10.8	(210)		
		9.52	9.5	(300)		
		<i>ca.</i> 7.8	—	<i>h</i> <sub>2</sub>		
		<i>ca.</i> 4.7	—	<i>a</i>		
<b>3e:</b> [(C <sub>16</sub> S) <sub>8</sub> Pc] <sub>2</sub> Lu (D <sub>h</sub> at 120 °C)	<i>a</i> = 35.1	30.4	30.4	(100)		
	<i>h</i> <sub>2</sub> = <i>ca.</i> 7.1	17.8	17.8	(110)		
		15.4	15.4	(200)		
		<i>ca.</i> 7.1	—	<i>h</i> <sub>2</sub>		
		<i>ca.</i> 4.7	—	<i>a</i>		
<b>3f:</b> [(C <sub>18</sub> S) <sub>8</sub> Pc] <sub>2</sub> Lu (D <sub>h</sub> at 100 °C)	<i>a</i> = 38.3	33.5	33.2	(100)		
	<i>h</i> <sub>2</sub> = <i>ca.</i> 7.0	19.2	19.1	(110)		
		16.5	16.6	(200)		
		12.3	12.5	(210)		
		<i>ca.</i> 7.0	—	H <sub>2</sub>		
		<i>ca.</i> 4.7	—	<i>a</i>		

<sup>a</sup>Halo of the molten alkythio chains.

of charge transport must be controlled mainly by the overlap between the  $\pi$ -systems of neighboring phthalocyanine units.

Particularly interesting for the present Lu compounds is the

lack of a substantial decrease in the mobility at the transition from the mesophase to the isotropic liquid. This indicates that there is still a considerable degree of columnar order in the



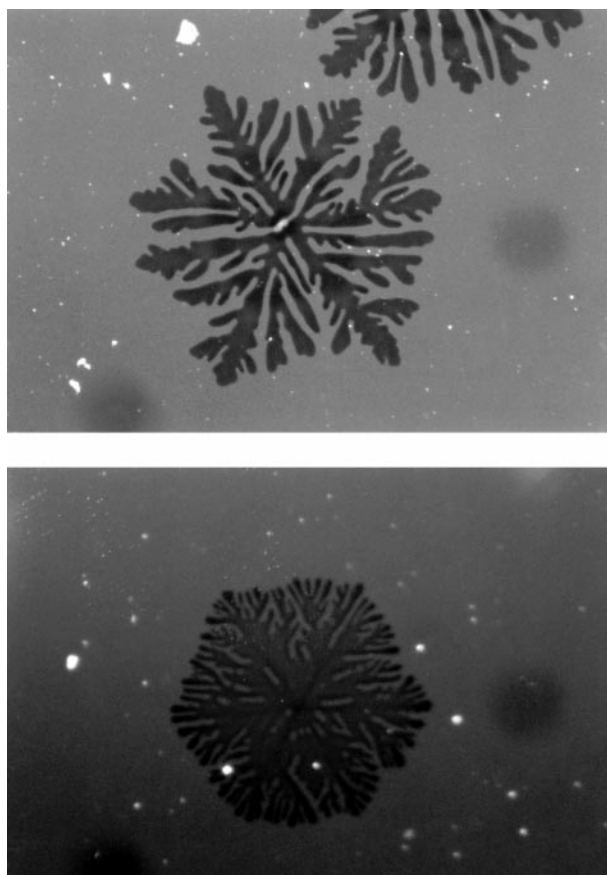


Fig. 2 Photomicrographs of  $[(C_{12}S)_8Pc]_2Tb$  (**2c**) at  $168^\circ C$ , recorded with uncrossed polarizers.

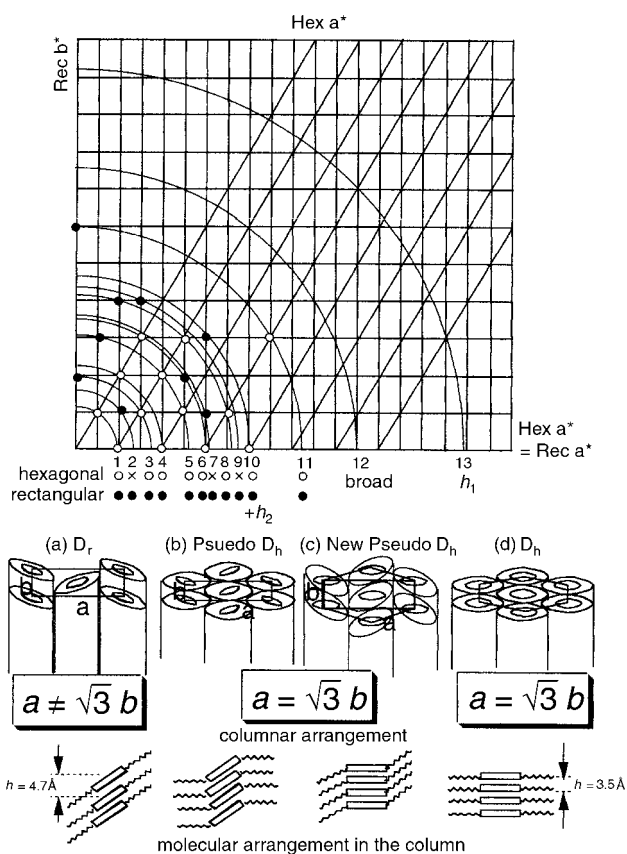


Fig. 3 The reciprocal lattices of hexagonal and rectangular symmetries of  $[(C_{12}S)_8Pc]_2Eu$  and schematic representations of discotic liquid crystalline phases of  $D_{rh}$ , pseudo  $D_{ho}$  and  $D_{ho}$ .

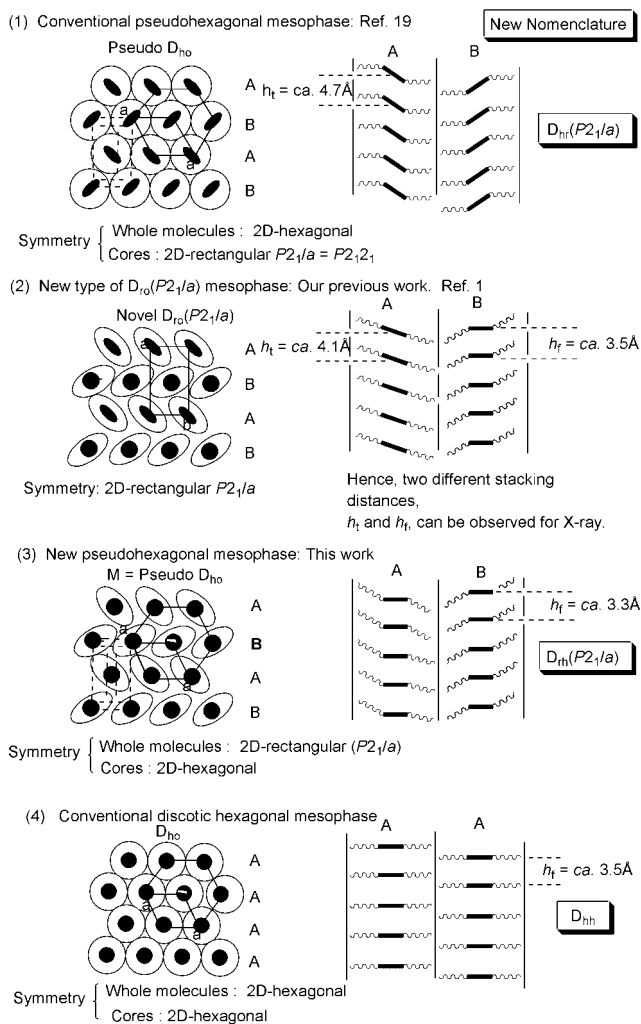
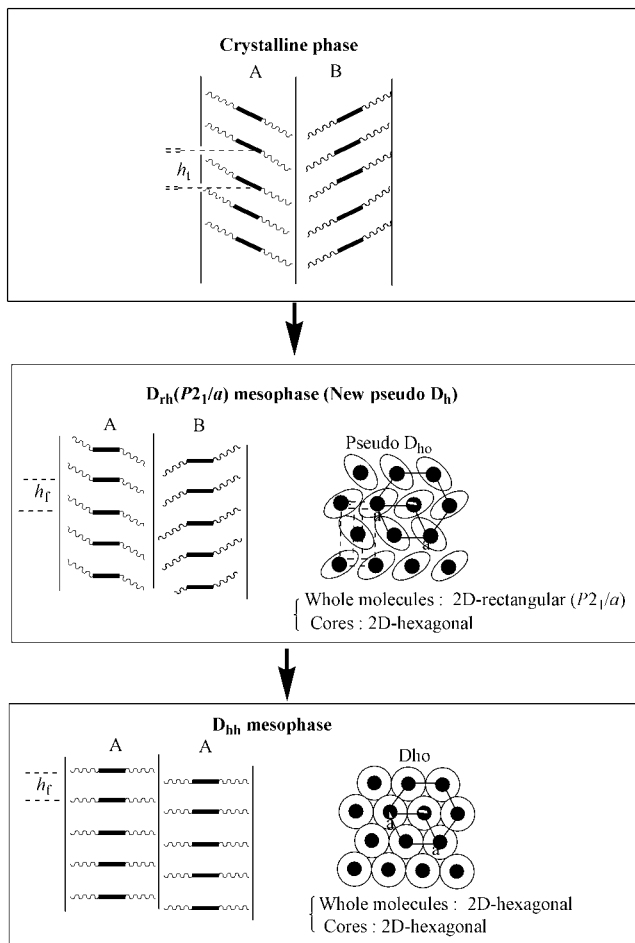


Fig. 4 Relationship between the two-dimensional columnar packing symmetry and the one-dimensional molecular stacking feature for four special columnar mesophases.

isotropic phase which allows the charge to move rapidly via intermolecular charge-transfer rather than by molecular ion diffusion. The dimeric Lu compounds may therefore be considered to be the first liquid phase organic semiconducting materials.

For the  $[(C_{12}S)_8Pc]_2Lu$  compound there is an indication of a slight decrease in  $\Sigma\mu_{1D}$  within the temperature range corresponding to the novel  $D_{rh}(P2_1/a)$  phase, the evidence for which was presented in previous sections. This decrease to a value of  $ca. 0.7\text{ cm}^2\text{ V}^{-1}\text{ s}^{-1}$  is, however, smaller than the eventual decrease found on entering the  $D_h$  phase. This indicates that in the  $D_{rh}(P2_1/a)$  phase the columnar stacks are still relatively rigid.

The results for the present  $[(C_nS)_8Pc]_2Lu$  derivatives differ considerably from those reported previously for the alkoxy substituted material,  $[(C_{12}O)_8Pc]_2Lu$ .<sup>7</sup> Firstly, the  $\Sigma\mu_{1D}$  values are much larger than those for the alkoxy derivative at all temperatures. In addition, there is a marked qualitative difference in that the alkoxy lutetium derivative displayed an abrupt increase in  $\Sigma\mu_{1D}$  at the transition from the crystalline solid to the higher temperature mesophases whereas the present compounds display an abrupt decrease. The increase in the case of  $[(C_{12}O)_8Pc]_2Lu$  was attributed to an abnormally low value of  $\Sigma\mu_{1D}$  in the crystalline solid phase rather than to an unusually high mobility in the mesophase. This is in agreement with the fact that the mobility in the K phase of  $[(C_{12}O)_8Pc]_2Lu$  is close to two orders of magnitude lower than that in the K phase of



**Fig. 5** Schematic representations of the changes in the mesophase structure for the  $[(C_nS)_8Pc]_2M$  ( $M=Eu, Tb, Lu$  and  $n=10, 12$ ) derivatives on heating.

$[(C_{12}S)_8Pc]_2Lu$ . This large difference is thought to be related to the adoption of a non-planar geometry of the phthalocyanine units in the former compound similar to that found for unsubstituted, crystalline  $Pc_2Lu$ . This could result in a higher degree of charge localization at the sandwich dimer sites and a larger distance between identical sites within the stack, *i.e.* 7 Å instead of 3.5 Å. This would have a large negative influence on the rate of intracolumnar charge carrier hopping. The large differences between the mobility in the K phases may therefore reflect a much smaller degree of puckering of the phthalocyanine macrocycles in the  $[(C_{12}S)_8Pc]_2Lu$  material.

#### 4 Conclusions

Novel phthalocyaninato rare-earth metal (Eu, Tb, Lu) sandwich complexes substituted with sixteen alkylthio chains have been synthesized and their mesomorphic and charge transport properties have been investigated.

A novel unique pseudo-hexagonal mesophase,  $D_{rh}(P2_1/a)$ , has been found for at least two compounds of each rare-earth derivative series,  $[(C_nS)_8Pc]_2Eu$  ( $n=10, 12$ ),  $[(C_nS)_8Pc]_2Tb$  ( $n=10, 12, 14$ ) and  $[(C_nS)_8Pc]_2Lu$  ( $n=10, 12$ ). This mesophase has a two-dimensional rectangular lattice for the whole molecules and a two-dimensional hexagonal lattice for the central core disks. The compounds studied are the first to show this mesophase in liquid crystals.

Replacement of sulfur for oxygen as the chain-to-core coupling element in peripherally hexadecaalkyl substituted  $Pc_2Lu$  derivatives results in an increase by more than an order of magnitude in the intracolumnar charge carrier mobility to values in the range 0.15 to 0.3  $cm^2 V^{-1} s^{-1}$  which is close to the

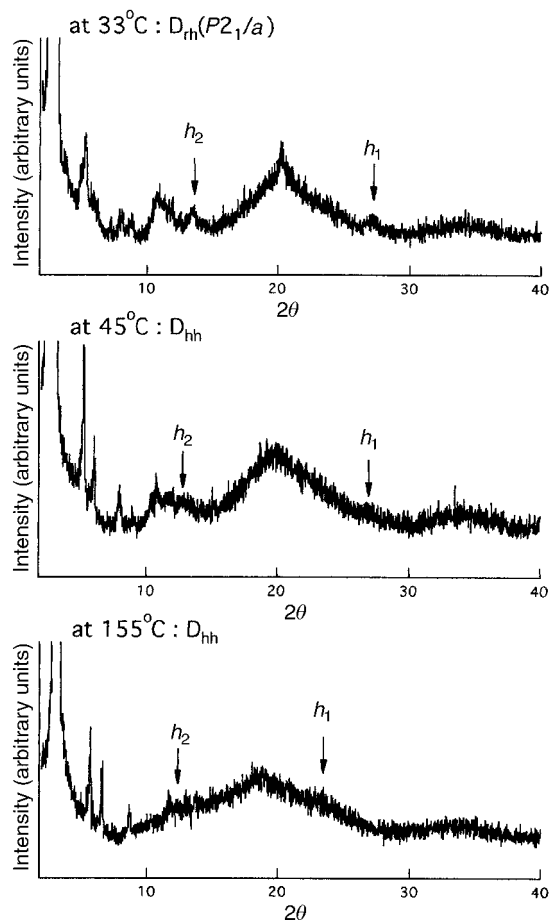


**Fig. 6** X-Ray diffraction patterns of the  $[(C_{12}S)_8Pc]_2Lu$  complex.

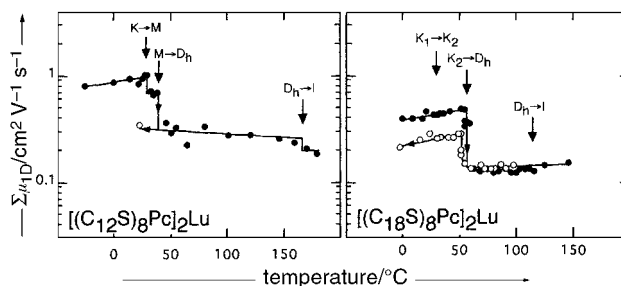


**Fig. 7** The temperature dependence of the one-dimensional, intracolumnar charge carrier mobility in  $[(C_{12}S)_8Pc]_2Lu$  and  $[(C_{18}S)_8Pc]_2Lu$  for the first heating trajectory (filled circles) and on cooling (open circles). The phase transition temperatures determined by DSC and polarization microscopy are also shown.

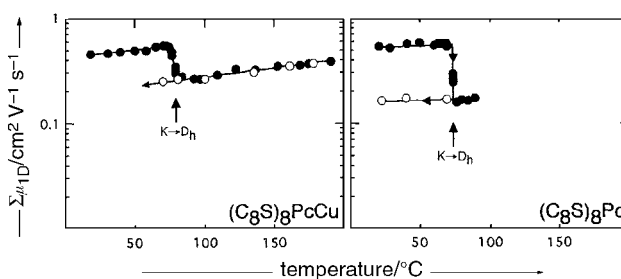


**Fig. 8** The temperature dependence of the one-dimensional, intracolumnar charge carrier mobility in  $(C_8S)_8PcCu$  and  $(C_8S)_8Pc$  for the first heating trajectory (filled circles) and on cooling (open circles). The phase transition temperatures determined by DSC and polarization microscopy are also shown.

maximum ever previously obtained for the  $D_h$  phase of discotic materials.<sup>8,21</sup> The mobility remains high in the isotropic liquid phase indicating that a high degree of columnar order still exists and allows charge transport to occur *via* intermolecular charge transfer rather than by molecular ion diffusion. The novel  $D_{rh}(P2_1/a)$  phase in  $[(C_{12}S)_8Pc]_2Lu$  displays a higher mobility (*ca.*  $0.7 \text{ cm}^2 \text{ V}^{-1} \text{ s}^{-1}$ ) than the  $D_h$  phase.

## Acknowledgements

This work was partially supported by Grant-in-Aid for Research (10CE2003 and 12129205) by the Ministry of Education, Science, Sports and Culture of Japan. We are grateful to Dr M. Kimura for mass spectroscopy measurements.

## References

- Part 28: R. Naito, K. Ohta and H. Shirai, *J. Porphyrins Phthalocyanines* in the press.
- J. Simon and J.-J. André "Molecular Semiconductors", Springer Verlag, Berlin, 1985; M. Hatano and H. Konami, *Senryou to Yakuhin*, 1991, **36**, 3.
- A. De Cian, M. Moussavi, J. Fischer and R. Weiss, *Inorg. Chem.*, 1985, **24**, 3162.
- T. Komatsu, K. Ohta, T. Watanabe, H. Ikemoto, T. Fujimoto and I. Yamamoto, *J. Mater. Chem.*, 1994, **4**, 537.
- C. Piechocki, J. Simon, J.-J. André, D. Guillon, P. Petit, A. Skoulios and P. Weber, *Chem. Phys. Lett.*, 1985, **122**, 124.
- Z. Belarbi, C. Sirlin, J. Simon and J.-J. André, *J. Phys. Chem.*, 1989, **93**, 8105.
- A. M. van de Craats, J. M. Warman, H. Hasebe, R. Naito and K. Ohta, *J. Phys. Chem. B*, 1997, **101**, 9224.
- A. M. van de Craats, P. G. Schouten and J. M. Warman, *Ekisho (J. Jpn. Liq. Cryst. Soc.)*, 1998, **2**, 12; A. M. van de Craats, *Charge Transport in Self-Assembling Discotic Liquid Crystalline Materials* PhD Thesis, Delft University Press, Delft University of Technology, Delft, The Netherlands, 2000.
- K. Ban, K. Nishizawa, K. Ohta and H. Shirai, *J. Mater. Chem.*, 2000, **10**, 1083.
- Y. Suda, K. Shigehara, A. Yamada, H. Matsuda, S. Okada, A. Masaki and H. Nakanishi, *Proc. SPIE Int. Soc. Opt. Eng.*, 1991, **1560**, 75.
- D. Wöhrle, M. Eskers, K. Shigehara and A. Yamada, *Synthesis*, 1993, 194.
- H. Eichhorn and D. Wöhrle, *Liq. Cryst.*, 1997, **22**, 643.
- H. Ema, Master Thesis, Shinshu University, Ueda, 1988, Chapter 7.
- H. Hasebe, Master Thesis, Shinshu University, Ueda, 1991, Chapter 5.
- P. G. Schouten, J. M. Warman, M. P. de Haas, J. F. van der Pol and J. W. Zwikker, *J. Am. Chem. Soc.*, 1992, **114**, 9028.
- P. G. Schouten, J. M. Warman and M. P. de Haas, *J. Phys. Chem.*, 1993, **97**, 9863.
- P. P. Infelta, M. P. de Haas and J. M. Warman, *Radiat. Phys. Chem.*, 1977, **11**, 353; J. M. Warman, M. P. de Haas and H. M. Wentinck, *Radiat. Phys. Chem.*, 1989, **34**, 581.
- P. G. Schouten, *Charge Carrier Dynamics in Pulse-Irradiated Columnar Aggregates of Mesomorphic Porphyrins and Phthalocyanines*, PhD Thesis, Delft University of Technology, Delft, The Netherlands, 1994.
- A. M. van de Craats, J. M. Warman, M. P. de Haas, D. Adam, J. Simmerer, D. Haarer and P. Schuhmacher, *Adv. Mater.*, 1996, **8**, 823.
- P. Weber, D. Guillon and A. Skoulios, *Liq. Cryst.*, 1991, **9**, 369.
- A. M. van de Craats, J. M. Warman, A. Fechtenkötter, J. D. Brand, M. A. Harbison and K. Müllen, *Adv. Mater.*, 1999, **11**, 1469–1472.